Presentation 6.4

A ROUTE-BASED FORECASTING MODEL OF ROAD SURFACE FRICTION AND SNOW/ICE CONDITIONS

Teruyuki Fukuhara[a], Akira Saida[b], Akihiro Fujimoto[c], Masato Tanaka[d]

[a] *Department of Civil Engineering, Hiroshima Research Institute of Technology, 2-1-1, Miyake, Saiki-ku, Hiroshima, Japan,* [b] *Civil Engineering Research Institute for Cold Region, Japan, 1-34, 1-jo 3-choume Hiragishi, Toyohira-ku, Sapporo, Japan* [c] *Department of Civil Engineering, University of Fukui, 3-9-1, Bunkyo, Fukui, Japan,* [d] *Misawa Environmental Technology Co. Ltd., 4252-2, Mukoueta, Miyoshi, Japan,*

t.fukuhara.ek@it-hiroshima.ac.jp

1. Introduction

Road surface friction ⍰ is an objective parameter to express the degree of driving risk. Obtaining ⍰ over a wide area in advance is an effective way to support flexible deployments of snow removal machines and necessary to minimize salt use without reducing winter road safety.

This study aims at proposing a route-based ⍰ forecasting model (SAFFII-model)) and evaluating the model accuracy by comparing the calculated road surface temperature (*RST*) and road resistance value (Halliday Friction Number, *HFN*) with the measured ones.

2. Road weather and heat balance theory

2.1 Heat balance of snow layer

The proposed forecasting model consists of the calculations of the road weather, *RST*, ice mass fraction of snow on a road surface, snow depth and *HFN*.

The heat balance of snow layer on the road surface is given by Eq. (1).

$$(\rho c)_s \frac{\partial (T_s h_s)}{\partial t} = q_{sds} + q_{lds} - q_{lus} + q_{as} + q_{sf} - q_{le} - q_{sa} + q_{lm} - q_{if} - q_{dr} + q_{sp} - q_{st} \qquad (1)$$

where, $(\rho c)_s$: volumetric heat capacity of snow layer, T_s: snow temperature, h_s: thickness of snow layer, t: time, q_{sds}: solar radiation flux$^{1)}$ (top surface layer, TSL), q_{lds}: incoming longwave radiation flux$^{1)}$ (TSL), q_{lus}: outgoing longwave radition$^{1)}$ (TSL), q_{as}: sensible heat flux due to vehicle induced or natural wind$^{1)}$ (TSL), q_{sf}: rain/snow sensible heat flux$^{2)}$ (TSL) , q_{le}: latent heat flux due to evaporation$^{2)}$ (TSL), q_{sa}: sensible heat flux associated with splash$^{2)}$, q_{lm}: latent heat flux due to melting or freezing$^{2)}$, q_{if}: sensible heat flux due to downward movement of meltwater$^{3)}$ (except bottom snow layer, BSL), q_{dr}: sensible heat flux due to drain (BSL), q_{sp}: heat flux between snow layer and road surface$^{2)}$ (BSL), q_{st}: solar radiation flux through the snow layer $^{2)}$.

2.2 Heat balance of road surface layer

A sudden change of snow condition due to snow removal is taken account in this theory. The heat balance of the road (pavement) surface layer contacting with the snow layer is given by Eq. (2).

$$(\rho c)_p \frac{\partial T_{ps}}{\partial t} dz_{ps} = -q_{sp} + q_p + q_{st} \qquad (2)$$

where, $(\rho c)_p$: volumetric heat capacity of pavement, T_{ps}: temperature of road surface layer, dz_{ps}: thickness of road surface layer and q_p: conductive heat flux in pavement.

3. Mass and volume balance theory of snow layer

3.1 Water mass balance

The time rate of water mass M_w in the snow layer is expressed by Eq. (3).

$$\frac{\partial M_w}{\partial t} = M_{fw} + M_{lw} + M_{iw} - M_{sw} - M_{dw} - M_{saw} \qquad (3)$$

where, M_{fw}: water flux due to rainfall $^{2)}$ (TSL), M_{lw}: water flux due to phase change $^{2)}$ (TSL), M_{iw}: ice flux due to melting or freezing $^{2)}$ (>0: melting, <0: freezing), M_{sw}: melt water flux$^{3)}$ (except BSL), M_{dw}: draining water flux (BSL) and M_{saw}: water flux reduced by splash.

3.2 Ice mass balance

The time rate of ice mass M_i in the snow layer is expressed by Eq. (4).

$$\frac{\partial M_i}{\partial t} = M_{fi} + M_{li} - M_{iw} - M_{sai} \qquad (4)$$

where, M_{fi}: ice flux due to snowfall$^{2)}$ (TSL), M_{li}: sublimation flux$^{2)}$ (TSL) and M_{sai}: ice flux reduced by splash.

3.3 Air volume balance

The time rate of air volume V_a in the snow layer is expressed by Eq. (5).

$$\frac{\partial V_a}{\partial t} = V_{fa} - V_{exa} - V_{oa} - V_{saa} - V_{vca} \qquad (5)$$

where, V_{fa}: air volume flux due to snowfall$^{2)}$ (TSL), V_{exa}: air volume flux replaced by water or ice due to melting or freezing$^{2)}$, V_{oa}: air volume flux reduced by snow-melting$^{2)}$ (TSL), V_{saa}: air volume flux reduced by splash and V_{vca}: air volume flux reduced by snow condensation$^{2)}$.

3.4 Sliding resistance and snow conditions

The sliding resistance of the snow layer is expressed by the *HFN*. The *HFN* is calibrated in a range of 0 to 80~100 (min: 0-slip ratio, max: dry road surface) and may be given as a function of the thickness of ice component in the snow layer as follows:

$$HFN = HFN_w - 86.8 + 64.8(\theta_i h_s)^{-0.154} \qquad (6)$$

where, HFN_w: *HFN* on wet road surface and ϑ_i: volumetric ice content.

4. Thermal and *HFN* mapping

Thermal-*HFN* mapping and meteorological survey were conducted over the 12.6 km section between Santo IC and Aogaki IC on the Kasuga-Wadayama Expressway in Hyogo prefecture, Japan. The *RST* and *HFN* were measured at intervals of approximately 2m by a vehicle equipped with a continuous friction tester (CFT).

5. Results and discussions

Fig. 1 (a) and 1 (b) show the comparison of the calculated and measured spatial variations in T_s and *HFN* at 02:00 and 06:30 on January 26, 2012, respectively. These data were obtained on slush and snow packed road surfaces. The calculated T_s, $T_{s\text{-}cal}$ was in good agreement with measured T_s, $T_{s\text{-}obs}$ (•) at two different times of the day.

Spikelike fluctuations of measured *HFN*, $HFN_{\text{-}obs}$ may include mechanical errors of the CFT on random rough snow surfaces. When the contact position of the CFT on the road surface deviates from the track of the tire in front of the CFT, the calculation accuracy of *HFN*□may become low. It is seen that the plots of $HFN_{\text{-}obs}$ (•) are scattered around the calculated lines as a series of plots of $HFN_{\text{-}cal}$ at two different times of the day. Significant changes in $HFN_{\text{-}cal}$ can be recognized at the mouths of tunnels as well as $HFN_{\text{-}obs}$.

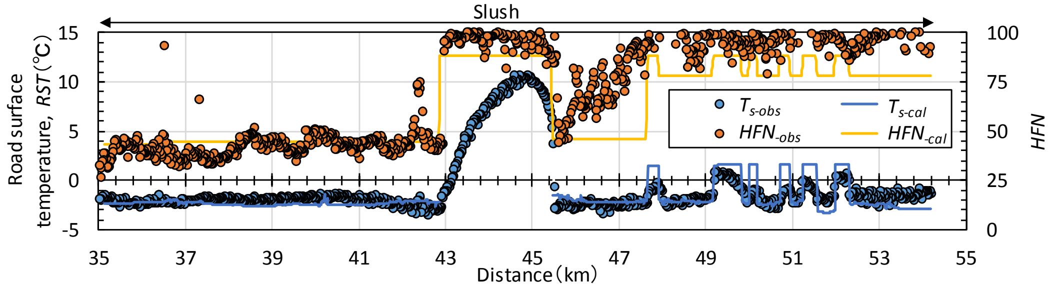

(a) 1/26 2:00

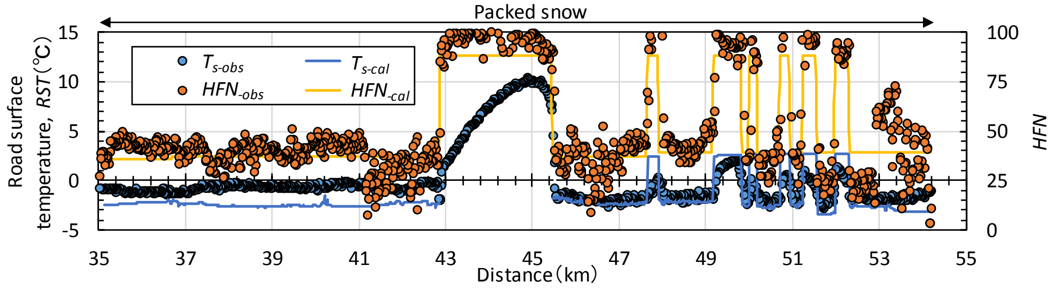

(b) 1/26 6:30

Fig. 1. *RST* and *HFN* distribution along the route (2012)

6. Conclusions

A route-based □ forecasting model (SAFFII-model) was proposed and the model accuracy was discussed in this paper. It is concluded that SAFFII-model could reproduce the spatial variations in the road surface temperature and Halliday Friction Number, *HFN* measured along the expressway.

References:

1) Saida, A. et al., **2013**, Forecasting model of road surface temperature along a road network by heat balance method, *Journal of Japan Society of Civil Engineers E1*, *69-2*, 1-11.

2) Fujimoto, A. et al, **2007**, Melting analysis of a thin snow/ice layer on road surface subjected to radiation-transmission, *Journal of Japan Society of Civil Engineers E*, *63-2*, 202-213.

3) Fujimoto, A. et al, **2008**, Multilayerd snow/ice model on road, *Journal of Snow Engineering of Japan*, *24-1*, 3-11.